Journal of Medicinal Chemistry

Article

pubs.acs.org/jmc

Retooling Manganese(III) Porphyrin-Based Peroxynitrite Decomposition Catalysts for Selectivity and Oral Activity: A Potential New Strategy for Treating Chronic Pain

Smita Rausaria,[†] Mahsa M. E. Ghaffari,[†] Andrew Kamadulski,[†] Kenny Rodgers,[‡] Leesa Bryant,[§] Zhoumou Chen,[§] Tim Doyle,[§] Michael J. Shaw,[‡] Daniela Salvemini,[§] and William L. Neumann*[,†]

[†]Department of Pharmaceutical Sciences, School of Pharmacy, and [‡]Department of Chemistry, Southern Illinois University, Edwardsville, Illinois 62026, United States

[§]Department of Pharmacology and Physiology, St. Louis University, St. Louis, Missouri 63104, United States

Supporting Information

ABSTRACT: Redox-active metalloporphyrins represent the most well-characterized class of catalysts capable of attenuating oxidative stress in vivo through the direct interception and decomposition of superoxide and peroxynitrite. While many interesting pharmacological probes have emerged from these studies, few catalysts have been developed with pharmaceutical properties in mind. Herein, we describe our efforts to identify new Mn(III)−porphyrin systems with enhanced membrane solubilizing properties. To this end, seven new Mn(III)-tetracyclohexenylporphyin (TCHP) analogues, **7**, **10**, **12**, **15**, and **16a−c**, have been prepared in which the *beta*-fused cyclohexenyl rings provide a means to shield the charged metal center from the membrane during passive transport. Compounds **7**, **15**, and **16a−c** have been shown to be orally active and potent analgesics in a model of carrageenan-induced thermal hyperalgesia. In addition, oral administration of compound **7** (10−100 mg/kg, n = 5) has been shown to dose dependently reverse mechano-allodynia in the CCI model of chronic neuropathic pain.

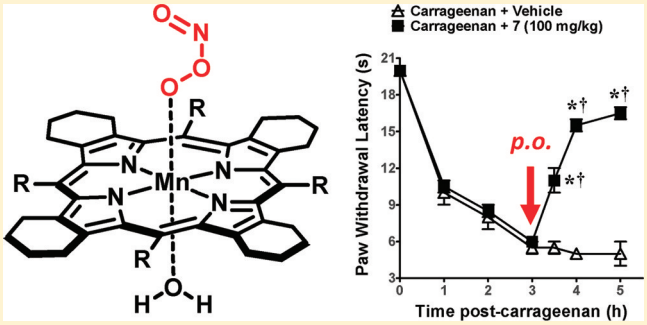

INTRODUCTION

Strategies that employ redox-active transition metal complexes for the in vivo catalytic detoxification of tissue-damaging reactive oxygen and reactive nitrogen species have shown great promise in animal and cell-based studies of diseases where oxidative stress plays a role.[1,2] To date, a number of catalytic antioxidant systems have been developed, with three of the most predominant classes represented by Mn(II) polyazamacrocycles, such as **1** (SC-72325; M40403);[3−5] Mn(III) ethylenebis(salicylimine) (Salens), such as **2** (Euk-134);[6] and Mn(III) and Fe(III) porphyrins, such as **3a** [Mn(III)-4-TMPyP^{5+}] and **3b** [Fe(III)-4-TMPyP^{5+}], respectively (Figure 1).[1,2] These classes vary significantly regarding their selectivity toward, and mechanisms of decomposition of, two critical mediators of oxidative and nitroxidative stress: superoxide and peroxynitrite (formed from the near diffusion-controlled reaction of superoxide and nitric oxide).[2] Most representatives of the Mn(II) polyazamacrocycle class have been reported as selective superoxide dismutase (SOD) mimics,[7,8] and Mn(III) Salens have been studied primarily as SOD/catalase mimics[9] [although Mn(III) Salens do react with peroxynitrite].[10] The Mn(III) and Fe(III) porphyrins are clearly the most versatile catalytic antioxidants from this group and have been studied primarily as dual SOD mimic/peroxynitrite decomposition catalysts (PNDCs).[1,2,11−13] It should also be noted that Mn(III) and Fe(III) corroles (the one carbon ring contracted derivatives of porphyrins) have also recently emerged as potent SOD mimic/PNDCs.[14−19]

As a result of the pioneering work of Fridovich[20−22] and subsequent development of the SOD mimic approach,[23] most current metalloporphyrin-based catalyst systems have been designed with an eye toward SOD activity first. The isomeric Mn(III)-tetrakis-(*meso*-*N*-alkylpyridinium)porphyrins [e.g., Mn(III)-4-TMPyP^{5+} **3a** and ortho-homologues **4a** and **4b**][1,11,12,24] are outstanding catalysts in this regard. These compounds dismute superoxide with some of the highest rate constants known for synthetic catalysts. The Fe(III) variants of these systems [i.e., Fe(III)-4-TMPyP^{5+}, **3b**] also possess excellent SOD activity.[1] The key design feature for SOD activity is the incorporation of highly electron-withdrawing *N*-alkylpyridinium groups in the *meso*-positions of the porphyrin macrocycle. For compounds such a Mn(III)-4-TMPyP^{5+} **3a** and related congeners, the metal-centered reduction potentials are subsequently adjusted to values that are nearly ideal for the rapid dismutation of superoxide.[1,25] Thus, the electron-deficient

Received: September 16, 2011
Published: November 14, 2011

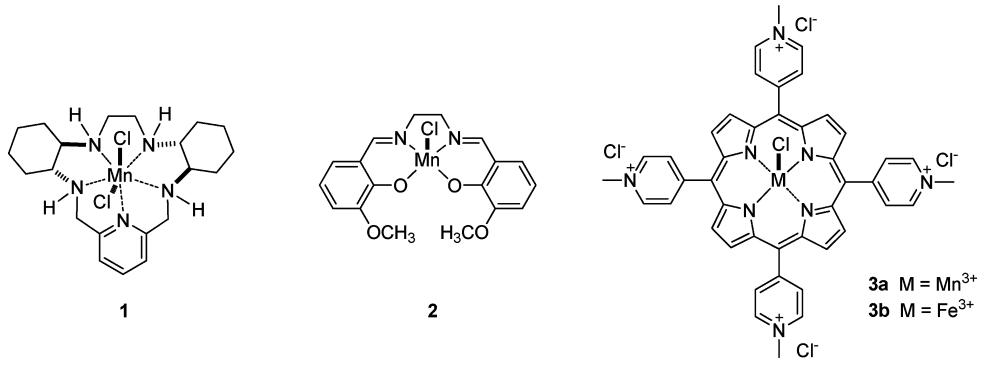

Figure 1. Transition metal-based catalytic antioxidants.

Scheme 1. SOD Activity (A) and PNR Activity (B) of Mn(III) Porphyrins

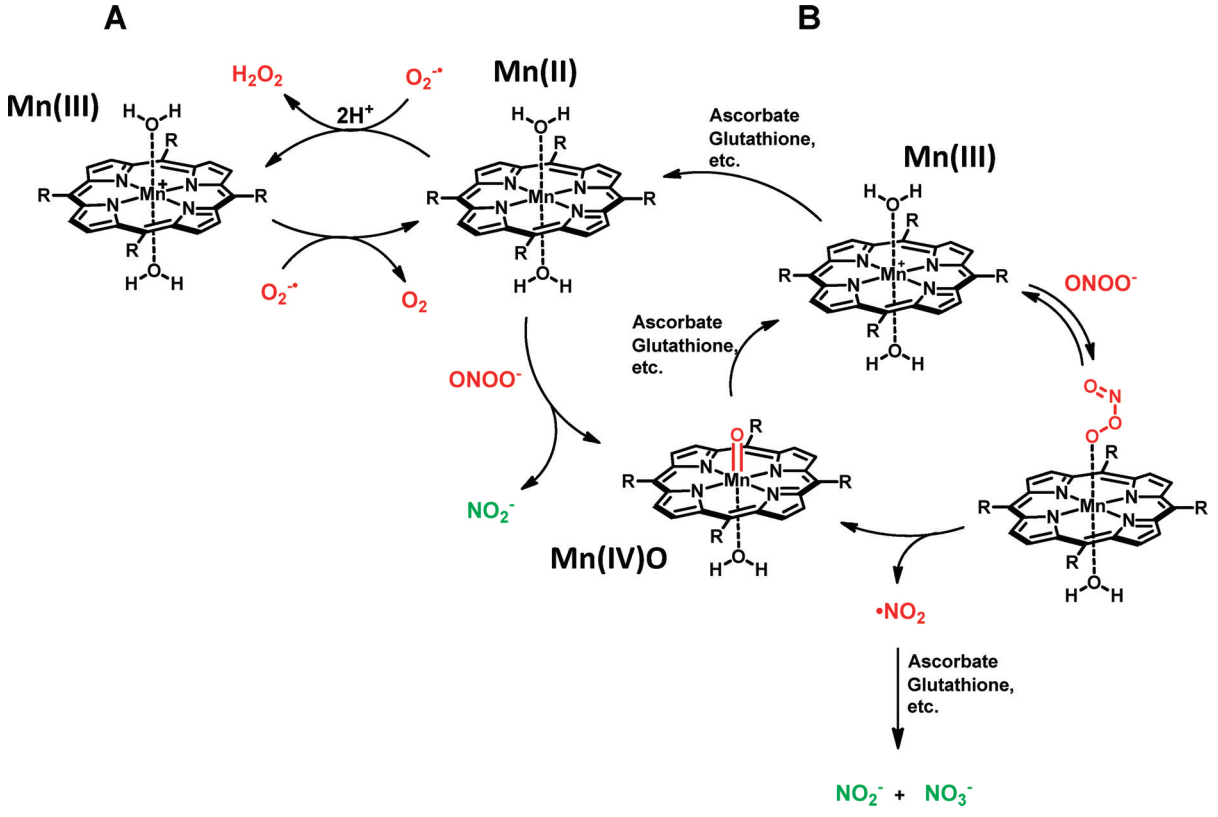

Mn(III) complex can be readily reduced to the Mn(II) form by superoxide, which is oxidized to molecular oxygen. The proton-dependent reoxidation of the Mn(II) form by superoxide reforms the Mn(III) complex and completes the dismutation process (and catalytic cycle) by producing hydrogen peroxide (Scheme 1A).[1,12]

In addition to SOD activity, compounds such as Mn(III)-4-TMPyP^{5+} **3a** have been shown to function as potent peroxynitrite reductases (PNRs).[1,12] The mechanism of action for these types of catalysts has been studied thoroughly by Groves[12] and involves an overall one-electron reduction of peroxynitrite to nitrogen dioxide with concomitant oxidation of the Mn(III) catalyst to the Mn(IV)O species. Endogenous coreductants such as ascorbate or glutathione have been shown to rapidly reduce both the potentially damaging nitrogen dioxide to nitrite and the Mn(IV)O species back to Mn(III).[11,12] This completes a reductase type catalytic cycle and detoxifies peroxynitrite (Scheme 1B, right cycle). Alternatively, electron-poor complexes can also reduce peroxynitrite via a two-electron process.[26,27] This pathway requires preliminary reduction of the Mn(III) catalyst to the Mn(II) form by cellular reductants, a process that is again contingent on having an electron-poor metal center. Reaction of the Mn(II) center with peroxynitrite can produce nitrite directly with concomitant oxidation of the Mn(II) form by two electrons, and oxygen atom transfer, to generate the Mn(IV)O species.[2,27] Cellular reductants would again be necessary to reduce the Mn(IV)O form and complete the reductase-like cycle (Scheme 1B, center cycle). The Fe(III)-based systems are also quite interesting regarding their reactivity with peroxynitrite in that they can function, at least partially, as isomerases by catalytically converting peroxynitrite to nitrate ion.[28]

In general, the emphasis of metalloporphyrin chemistry research programs in these areas has primarily been on optimizing catalytic activity and further elucidating the mechanisms of catalysis. To this end, some very impressive

dx.doi.org/10.1021/jm201233r | J. Med. Chem. 2011, 54, 8658–8669

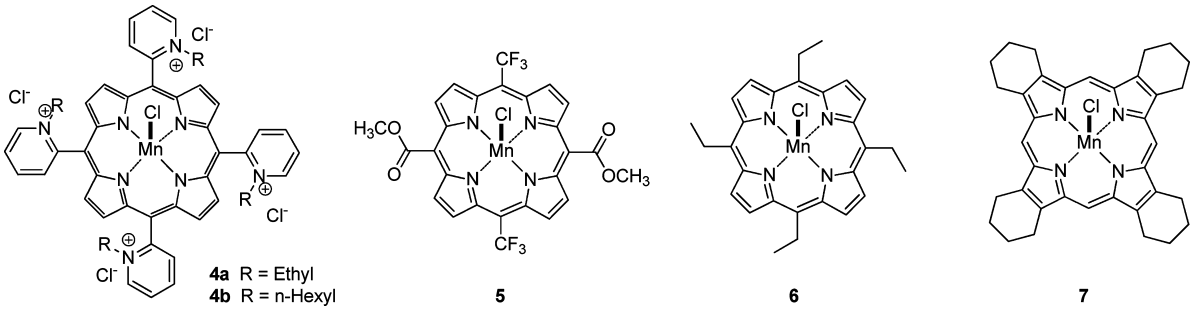

Figure 2. Membrane-soluble catalytic antioxidants.

and comprehensive studies have been reported that correlate rates of catalysis with reduction potential of the metal center (for SOD activity),[29] rates and mechanism of catalysis with secondary coreductant (PNR activity),[11,12,30] and rates of catalysis with number and proximity of positive charges (electrostatic guidance for both SOD and PNR activity).[1,30,31] However, thus far, only a limited number of studies have been concerned with enhancing the druglike properties of the catalyst beyond the functional metal center. Attempts to increase the lipophilicity and membrane solubility of compounds related to Mn(III)-4-TMPyP^{5+} **3a** through regiochemical variations and homologation of the alkylpyridinium substituents have met with some success, yielding compounds like Mn(III)-2-TE-PyP^{5+} **4a** and Mn(III)-2-TnHex-2-PyP^{5+} **4b** (Figure 2).[32−34] These compounds are extremely interesting catalysts and have shown improved cellular and subcellular penetration.[32,35] Other intriguing studies have shown that further modification of *meso*-substituents can in fact yield complexes that are orally active. In this regard, Mn(III)-5,15-bis(methoxycarbonyl)-10,20-bis-trifluoromethylporphyrin[36] **5** and Mn(III)-5,10,15, 20-tetraethylporphyrin[37] **6** are examples of orally active porphyrins that have been reported as SOD mimics with catalase activity.

Our desire to identify PNR catalyst scaffolds with oral bioavailability was motivated by our continued interest in the role of peroxynitrite in inflammatory and neuropathic pain.[38−40] Thus, orally active and preferably selective PNR catalysts were needed as pharmacological probes for in vivo studies of these chronic pain conditions and also to potentially serve as therapeutic lead scaffolds for translational studies. In looking through the literature, we were drawn to the significant recent advances that have been made in the construction of highly functionalized porphyrin systems for use in the areas of materials science,[41−43] nonlinear optics,[44,43] optical imaging and sensing,[45−48] and photodynamic therapy.[47,49] Because in a number of studies porphyrin systems were designed to be highly lipophilic for various materials applications (e.g., films[50]), we thought this might be fertile territory to mine for membrane-soluble catalyst ideas. One particular porphyrin scaffold, used primarily as a synthetic intermediate, that stood out from the others was the symmetric hexahydro-29*H*,31*H*-tetrabenzo[*b*,*g*,*l*,*q*]porphine (hereafter referred to as tetracyclohexenylporphyrin, TCHP).[45,51,52] We have used similar cyclohexyl and cyclohexenyl substitutions in previous studies of Mn(II) polyazamacrocycles (as SOD mimics) for both conformational control of metal chelation and to impart membrane solubilizing character to the complex for enhanced bioavailability.[4,53,54] Other lipophilic fused-ring porphyrin systems (of geochemical interest)[52] may also be useful for catalyst development, but we settled upon the TCHP scaffold for these studies as it accomplishes our design strategy and is readily prepared.

Thus, we hypothesized that the Mn(III)-TCHP complex **7** would afford a monocationic metalloporphyrin system in which the symmetric zones of lipophilicity afforded by the *beta*-fused cyclohexenyl substitution would effectively "shield" the polar region of charge on the metal center from the membrane (during passive transport and oral absorption). This idea is analogous to the charge-shielded membrane transport component of ionophore activity (e.g., the high lipid solubility of the valinomycin-potassium ion complex).[55] Furthermore, it is now recognized that in addition to lipid solubility and global reduction of polar surface area, molecular rigidity, as estimated by the number of rotatable bonds, is another strong contributor to oral bioavailability.[56] These factors tend to be more important than molecular weight in predicting oral absorption.[56] Thus, we proposed that rigidifying hydrophobic functionality such as the fused cyclohexenyl groups of Mn(III)-TCHPs may contribute effectively to oral bioavailability in these types of systems. To test our hypothesis, a series of Mn(III)-TCHPs of varying lipophilicity (compounds **7**, **10**, and **12**) and with varying functionality (**15** and **16a−c**) were prepared, characterized, and evaluated in vivo as orally active PNR catalysts in models of inflammatory and neuropathic pain.

CHEMISTRY

To determine whether our metal charge-shielding structural paradigm based upon the TCHP scaffold would provide catalysts with enhanced druglike properties, we prepared a preliminary set of three compounds with varying degrees of *meso*-substitution. Thus, the readily available 2-ethoxycarbonyl-4,5,6,7-tetrahydro-2*H*-isoindole[51,52,57] **8** (Scheme 2) was prepared via the Barton-Zard reaction[58] from 1-nitrocyclohexene and ethyl isocyanoacetate as described in the literature.[51,52,57] Compound **8** was then converted to bis(4,5,6,7-tetrahydro-2*H*-isoindolyl)methane **9** by reaction with dimethoxymethane in acidic media followed by basic hydrolysis and decarboxylation at high temperature.[45] Dipyrromethane **9** was then converted to the Mn(III)-TCHP **7** by reaction with formaldehyde in refluxing acetic acid under aerobic conditions to form the ligand followed by complexation with $MnCl_2$ and in situ oxidation to the Mn(III) complex under basic aerobic conditions. The ligand system for Mn(III)-5,15-diphenyl-TCHP **10** was prepared by the method reported by Vinogradov and Cheprakov.[45] Thus, dipyrromethane **9** was allowed to react with benzaldehyde mediated by TFA followed by oxidation of the protoporphyrin system with DDQ. Mn(III) complex **10** was prepared by reacting the corresponding porphyrin ligand with $MnCl_2$ using the same procedure as that used to form complex **7**. Finally, the ligand system for

dx.doi.org/10.1021/jm201233r | J. Med. Chem. 2011, 54, 8658−8669

Scheme 2. Synthesis of Mn(III)-TCHPs with Varying Levels of *meso*-Substitution[a]

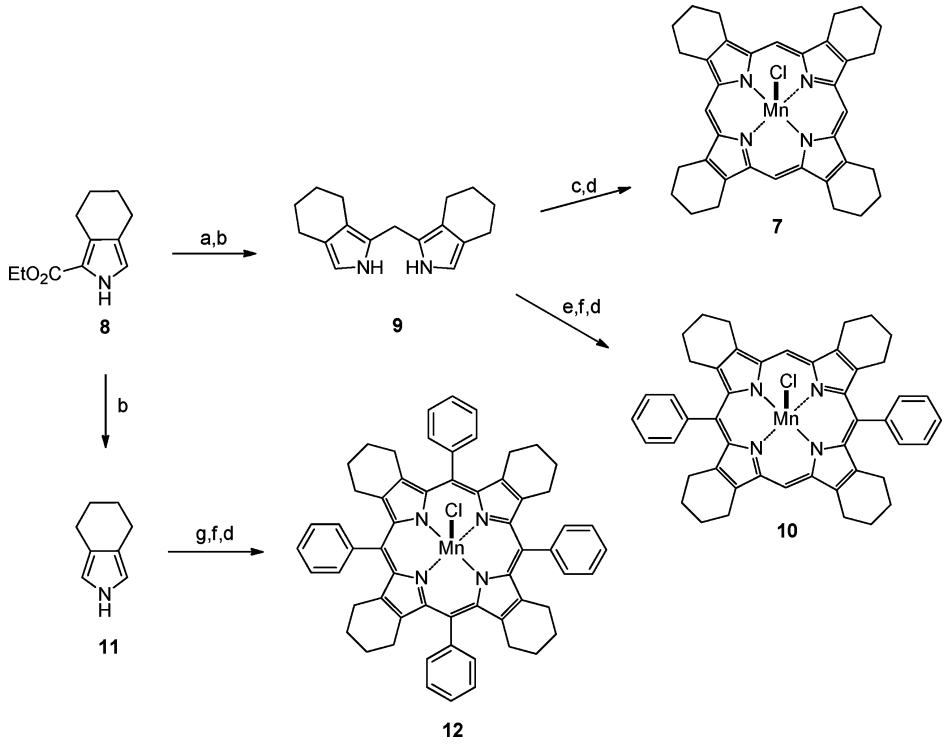

[a]Reagents and conditions: (a) $CH_2(OCH_3)_2$, *p*-TsOH, AcOH, 95%. (b) $(CH_2OH)_2$, KOH, 195 °C, 80%. (c) CH_2O, AcOH, reflux. (d) $MnCl_2$, $CHCl_3$, CH_3OH, 2,6-lutidine, air, 80%. (e) PhCHO, cat. TFA, CH_2Cl_2. (f) DDQ, CH_2Cl_2, 15% for two steps (from e). (g) PhCHO, $BF_3{\cdot}OEt_2$, CH_2Cl_2, 50%.

Mn(III)-5,10,15,20-tetraphenyl-TCHP **12** was prepared by another method reported in the literature.[59] Thus, compound **8** was hydrolyzed and decarboxylated in one pot to tetrahydroisoindole **11**.[45,59] This somewhat unstable compound was then allowed to react with benzaldehyde mediated by $BF_3{\cdot}OEt_2$, followed again by oxidation of the protoporphyrin system with DDQ. Mn(III) complex **12** was prepared exactly as described for complexes **7** and **10** above.

The octanol−water partition coefficients (Log *P* values) for these three Mn(III) TCHP complexes were measured by the slow stir method,[60] and the results indicated high lipid solubility (Table 1). Complex **7** afforded a Log *P* = 3.77, while bis-*meso*-phenyl analogue **10** afforded a Log *P* = 2.78. The lower Log *P* value for compound **10** may be due to the known deviation from planarity of deca- and doceca-substituted porphyrin ring systems.[61] To reduce steric interactions between the cyclohexenyl groups and the *meso*-phenyl substituents, the normally planar porphyrin undergoes a conformational saddling distortion, which may provide slightly more solvent access to the cationic Mn(III) center than in the non-*meso*-phenyl-substituted analogue **7**. This effect may serve to expose the Mn(III) center in compound **10** to solvent to a greater extent than the more planar and therefore more fully charge-shielded complex **7**. The addition of two more *meso*-phenyl groups resulting in the tetraphenyl-TCHP complex **12** afforded a Log *P* > 5, most likely due to the addition of lipophilicity in all *beta*- and *meso*-positions.

Mn(III)-5,15-diphenyl-TCHP **10** was chosen for further synthetic elaboration due to its intermediate lipophilicity and the ease with which the two *meso*-phenyl groups could be functionalized. Thus, 5,15-bis(4-methoxycarbonylphenyl)-TCHP **13** was prepared according to the method of Vinogradov and Cheprakov.[45] The esters were reduced to the bis-*meso*-benzyl alcohol derivative **14** in good yield using $LiAlH_4$. Complexation with $MnCl_2$ under aerobic basic conditions as before afforded the bis-*meso*-benzyl alcohol-functionalized Mn(III)-TCHP **15**. This complex then served as the key intermediate for the postchelate synthesis of three new reversed ester complexes **16a−c** by reaction with the appropriate anhydride in DMF (Scheme 3). We were unsuccessful in measuring the Log *P* values for compounds **15** and **16a−c** due to severe emulsion problems using standard octanol/water systems. Thus, these compounds were evaluated in terms of relative lipophilicity by determination of their respective reversed phase high-performance liquid chromatography (RPHPLC) retention factors (longer retention = greater lipophilicity)[62] as a mixture under isocratic conditions. This study revealed that the bis-*meso*-alcohol derivative **15** is substantially less lipophilic than parent compound **7** (measured Log *P* = 3.77), while the bis-*meso*-acetate **16a**, the bis-*meso*-propionate **16b**, and the bis-*meso*-isobutyrate **16c** are progressively more lipophilic (Figure S1 in the Supporting Information).

RESULTS AND DISCUSSION

Inhibition of Aryl Boronic Acid Oxidation Assay for Peroxynitrite Decomposition Activity. To evaluate the effectiveness with which each complex could intercept and decompose peroxynitrite, we needed a moderate throughput assay in which conditions could be easily varied with replicate runs. All complexes and known standards were therefore assayed for their ability to inhibit aryl boronate oxidation. The oxidation of 4-acetylphenylboronic acid to phenol, by attack of peroxynitrite on the electrophilic boron atom followed by

dx.doi.org/10.1021/jm201233r | J. Med. Chem. 2011, 54, 8658−8669

Table 1. Inhibitory Effects of Mn(III)-TCHPs on the Peroxynitrite-Mediated Oxidation of 4-Acetylphenylboronic Acid

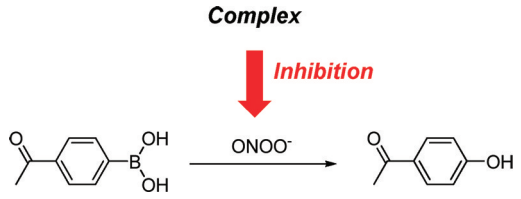

Catalyst Number	Structure	LogP[a]	% Inhibition (25 °C)
7	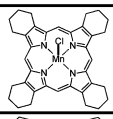	3.77	30 ± 2.5
10		2.78	22.3 ± 0.8
12	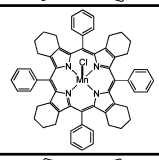	>5	14.6 ± 1.7
15	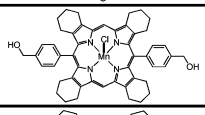	ND[b]	36.3 ± 2.5
16a	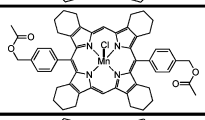	ND[b]	44.9 ± 4.2
16b	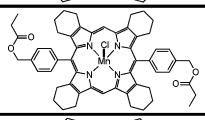	ND[b]	36.0 ± 3.0
16c	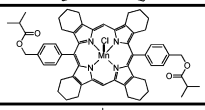	ND[b]	50.4 ± 5.8
3a	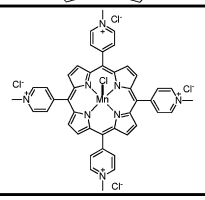	-4.54	62.4 ± 0.68

[a]Measured by the slow stir method.[60] [b]ND = not determined due to severe emulsion formation (see the Supporting Information for the evaluation of lipophilicity by HPLC).

rearrangement, is a clean conversion, and the second-order rate constant for this reaction has been accurately measured to be $k = 1.6 \times 10^6$ M^{-1} s^{-1} using stopped flow methods.[63] The extent to which a given Mn(III)-TCHP complex could inhibit this reaction would be a direct measure of the ability of the complex to compete with the aryl boronate for peroxynitrite. Thus, in effect, this method allows a crude estimation of the apparent second-order rate constant of the reaction of the complex with peroxynitrite based upon its ability to compete with the known boronate reaction. Under conditions of low peroxynitrite concentrations in vivo,[64,65] the second-order rate constant for the rate-limiting oxidation of a Mn(III) complex to the Mn(IV)O form with concomitant decomposition of peroxynitrite defines the efficiency of the process.[11,12] If endogenous reductants are plentiful, and their reduction of the Mn(IV)O form back to the resting Mn(III) complex is fast, a reductase catalytic cycle is enforced.[11,12] Under these conditions, the second-order rate constant for oxidation of Mn(III)-TCHPs is also the catalytic rate constant for the reductase cycle. Inhibition results for all Mn(III)-TCHP complexes, as well as the known compound Mn(III)-4-TMPyP^{5+} **3a**, are presented in Table 1. The known PNR catalyst Mn(III)-4-TMPyP^{5+} **3a** showed a 62.4% inhibition. From this value, we calculated the apparent second-order rate constant for the oxidation of the Mn(III) form of **3a** to the Mn(IV)O form to be $k = (2.6 \pm 0.2) \times 10^6$ M^{-1} s^{-1}, which is in close agreement with value measure by stopped-flow kinetic methods.[12,66] Thus, this assay provides a convenient method for the rapid, approximate in vitro measurement of activity toward the decomposition of peroxynitrite prior to in vivo studies. All compounds were to some extent effective at intercepting peroxynitrite and inhibiting boronate oxidation. Estimated apparent second-order rate constants for the Mn(III)-TCHPs are in the range of 10^5 to 10^6 M^{-1} s^{-1}. These are very respectable values given the monocationic nature of our Mn(III)-TCHPs, as electrostatic guidance has been invoked as being partially responsible for the efficiency with which polycationic complexes such as **3a** catalyze the decomposition of the peroxynitrite anion and superoxide radical anion.[1,31]

Electrochemistry and SOD Activity. As mentioned above, the removal of electron-withdrawing *meso*-substituents and the addition of the weakly inductive electron-donating cyclohexenyl groups result in Mn(III)-TCHP complexes that are substantially more electron rich than MnTE-2-PyP^{5+} (and related congeners). The electrochemistry of complex **10** was studied as a representative example of the behavior of this series of Mn(III)-TCHP charge-shielded catalysts in nonpolar solvents to mimic membrane space compartmentalization. Complex **10** features a cyclic voltammetry response in CH_2Cl_2, which includes a reversible (presumably porphyrin-based) oxidation at 0.89 V vs ferrocene and a chemically reversible Mn(II/III) couple at −0.79 V vs ferrocene. The latter features a much broader peak separation than the former, which is consistent with CV observations on other Mn (III)-porphyrin complexes. The increased peak separation is consistent with a fast follow-up reaction where the axial halide ligand is lost from the Mn(III) atom's coordination sphere upon reduction.

The conversion of nonaqueous measurements to the NHE scale (for comparison to polar water-soluble/membrane-insoluble catalysts such as MnTM-4-PyP^{5+}) is complicated by consideration of junction potentials and other problems.[67] There are multiple reports of the value of $E°'$ for ferrocene vs NHE, which range from −0.4 to −0.6 V vs NHE.[67] Using this range to convert our observed value for the Mn(II/III) couple to the NHE scale, it appears that the reduction potentials for Mn(III)-TCHP **10** and related complexes in this series are between −0.2 and −0.4 V. These estimates are consistent with the reports of $E°'$ values for Mn(II/III) couple for a number of 5- and 6-coordinate tetraphenylporphyrin complexes of manganese, which range from −0.43 to −0.54 V vs NHE.[68] In addition, these values confirm the electron-rich nature of the Mn(III)-TCHP complexes reported herein. Thus, the metal-based reduction potentials of Mn(III)-TCHPs will be out of the range useful for SOD activity (with +0.30 V optimal for high SOD activity).[1] Accordingly, our design concept for enhancing druglike properties and facilitating membrane penetration also

dx.doi.org/10.1021/jm201233r | J. Med. Chem. 2011, 54, 8658–8669

Scheme 3. Synthesis of Mn(III)-TCHPs with Alcohol and Ester Functionality[a]

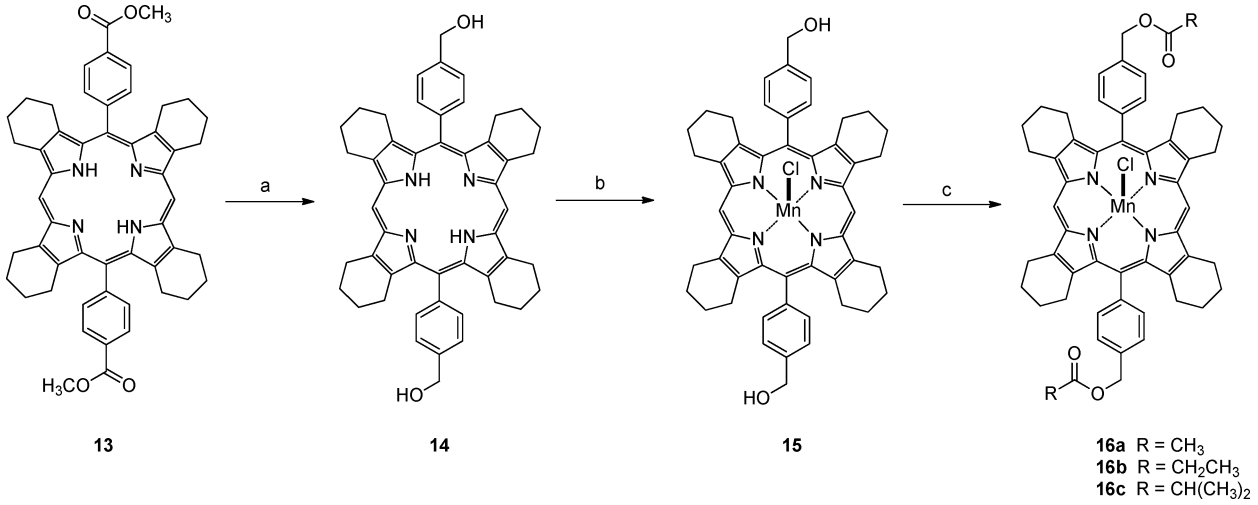

[a]Reagents and conditions: (a) $LiAlH_4$, THF, 80%. (b) $MnCl_2$, $CHCl_3$, CH_3OH, 2,6-lutidine, air, 74%. (c) Ac_2O, DMF, 91%; propionic anhydride, DMF, 84%; isobutyric anhydride, DMF, 85%.

limits SOD activity. Data comparing the measured SOD activity of complex 7 versus known SODm FeTM-4-PyP^{5+} using the xanthine/xanthine oxidase-luminol assay[69] are plotted in Figure 3.

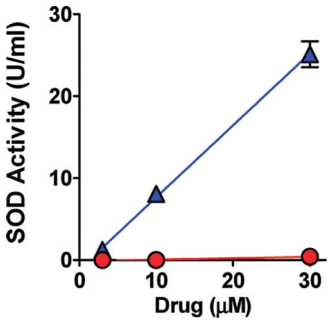

Figure 3. SOD activity of Mn(III)-TCHP 7. FeTMPyP^{5+} (▲), but not Mn(III)-THCP 7 (●), has potent SOD activity; $P < 0.001$ by linear regression analysis, $n = 3$ at each concentration.

Clearly, complex 7 shows only minimal SOD activity, while FeTM-4-PyP^{5+} potently inhibits superoxide-mediated oxidation of luminol. Peroxynitrite, however, is an extremely strong oxidant ($ONOO^-$, $2H^+/{}^{\bullet}NO_2$ $E^{o\prime} = 1.4$ V and $ONOO,2H^+/NO_2^-$ $E^{o\prime} = 1.2$ V)[70] and is reactive with most metalloporphyrins, as reflected by the boronate oxidation assay inhibition results for 7 and all Mn(III)-THCP complexes. Interestingly, sparing superoxide may actually be beneficial for physiological signaling,[71] and selectivity for peroxynitrite will be of great value in sorting out mechanistic pharmacological details regarding which reactive oxygen/nitrogen species (superoxide vs peroxynitrite) is the linchpin toxic species. Thus, our design concept originally aimed at enhancing druglike properties has affordeded PNR complexes with both enhanced lipid solubility (as reflected by their Log *P* values and/or their RPHPLC retention factors) and selectivity toward the decomposition of peroxynitrite. While complex 7 shows inhibition in the aryl boronate oxidation assay, which is roughly one-half that of highly cationic catalysts such as Mn-TE-2-PyP^{5+}, it is greatly enhanced membrane solubility compensates for this lower activity (in vivo results, next section). Previous studies with SOD mimics have described a modest version of such an effect in which less potent but more lipophilic complexes are equally effective in vivo as their related analogues with much greater activity but 10-fold lower lipophilicity.[1,33] The Log *P* of compound 7 is many orders of magnitude greater than both Mn-TM-4-PyP^{5+}, its homologated isomer MnTE-2-PyP^{5+}, and even long-chain N-alkyl analogues which still show negative values.[1,33]

Carrageenan-Induced Hyperalgesia. Intraplantar injection of carrageenan in rats leads to the time-dependent development of edema and thermal hyperalgesia.[72] This inflammatory response has been correlated with high levels of peroxynitrite flux as determined by the detection of nitrotyrosine formation and the effectiveness of PNDCs and inhibitors of peroxynitrite formation in treating the ensuing inflammation.[38−40,73,74] In addition to its potent pro-inflammatory and pro-apoptotic effects, the peroxynitrite-derived nitration and modification of protein functions essential for normal neuronal homeostasis are key disrupting factors that contribute to the mechanisms of hyperalgesia.[38−40]

As can be seen in Figure 4, whereas Mn(III)-TE-2-PyP^{5+} or Mn(III)-TCHP 7 blocked the development of carrageenan-induced hyperalgesia when given systemically by ip injection (10 mg/kg, $n = 3$), only 7 is able to block hyperalgesia when given orally by gavage (100 mg/kg, $n = 3$). The 100 mg/kg dose was used as a screening dose for oral activity before measuring the absolute oral bioavailability of promising lead molecules. In fact, postmortem evaluation of the animals revealed a substantial amount of the dark red complex 7 left in the gut (in precipitated form). Thus, a much smaller fraction of the 100 mg/kg dose was actually absorbed and therefore responsible for the pharmacological activity in this demanding assay. This is consistent with the great potential of a catalytic drug strategy. Nearly 100% inhibition is seen for 2 h with a substantial inhibitory effect maintained out to 5 h. It is noteworthy to mention that to achieve a similar degree of inhibition (at the 2 h time point) with the nonselective cyclooxygenase (COX)-1/COX-2 inhibitor ibuprofen, a dose of 300 mg/kg was required (99 ± 5% inhibition, $n = 6$, $P < 0.05$ as compared to carrageenan alone). Under the same conditions and at a dose of 300 mg/kg, acetaminophen or aspirin

dx.doi.org/10.1021/jm201233r | J. Med. Chem. 2011, 54, 8658−8669

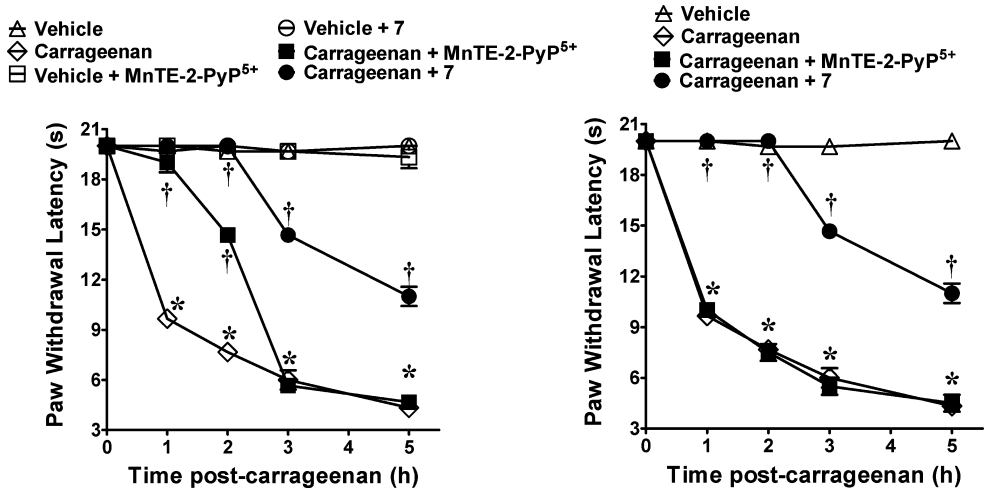

Figure 4. Inhibition of carrageenan-induced hyperalgesia by Mn(III)-TE-2-PyP^{5+} **4a** and Mn(III)-TCHP **7**. Systemic (ip) injection (left panel). Oral gavage (right panel). *P < 0.001 vs Veh, and $^{\dagger}P$ < 0.001 vs carrageenan.

attenuated hyperalgesia by 20 ± 4 and 50 ± 6%, respectively (n = 6, P < 0.05 as compared to carrageenan alone at the 2 h time point). Finally, ip injection of Mn(III)-TE-2-PyP^{5+} at a dose 2-fold higher than the one required to block hyperalgesia by some 90−100% by the ip route led to severe toxicities (lethargy and piloerection); 100% mortality was seen with a 3-fold higher dose. In contrast, no observable acute toxicities were noted with doses of complex **7** at least 6−8-fold higher than the one needed to block hyperalgesia to the same extent. While compounds **10** and **12** were also active at inhibiting hyperalgesia in this model, we have discontinued work on compounds from the dodecasubstituted series (e.g., **12**) due to insolubility. The evaluation of chronic toxicity for further optimized analogues within this class will be the subject of future studies.

In addition to the prophylactic treatment and thus prevention of carrageenan-induced hyperalgesia, complex **7** is able to reverse established hyperalgesia when dosed therapeutically. Thus, as shown in Figure 5, complex **7** (100 mg/kg) was

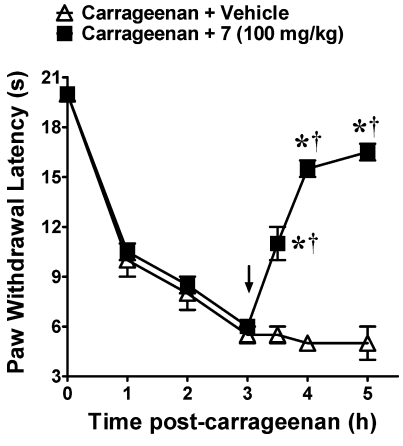

Figure 5. Reversal of carrageenan-induced hyperalgesia by oral administration of Mn(III)-TCHP **7**. *P < 0.001 vs Veh, and $^{\dagger}P$ < 0.001 vs carrageenan.

dosed orally by gavage at the time of maximal hyperalgesia (3 h postcarrageenan treatment). Within 1 h (4 h time point), pain was substantially reduced and at 2 h after dosing **7** (5 h time point), and paw withdrawal latencies were increased to approximately 90% of precarrageenan values.

Following our encouraging results with the Mn(III)-TCHP parent system **7**, we chose compound **10** for further structure−activity relationship (SAR) work, as it affords two *trans-meso*-phenyl substitutents, which are easily analogued (as described above in the Chemistry section). To this end, we prepared bis-*meso*-benzyl alcohol compound **15** originally for greater solubility and **16a−c** to modulate the in vivo performance of **15** through a prodrug type approach. Thus, bis-acetate **16a** was designed to potentially hydrolyze in vivo to **15** rapidly, while **16b** and **16c** would be increasingly resistant to esterase-mediated hydrolysis, respectively.[75] Results in the carrageenan assay for this series of compounds are presented in Figure 6. All

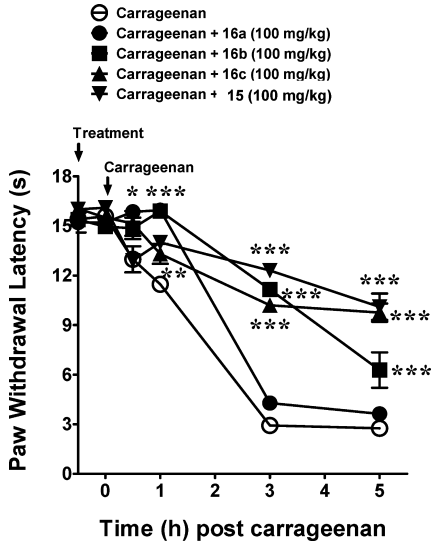

Figure 6. Inhibition of carrageenan-induced hyperalgesia by Mn(III)-TCHPs **15** and **16a−c**. *P < 0.05, **P < 0.01, and ***P < 0.001 vs carrageenan.

four compounds are effective in reducing hyperalgesia when dosed orally (100 mg/kg, n = 2). On the basis of known rates of hydrolysis for α-substituted esters (acetate > propionate > isobutyrate)[75] and previous experience with lipophilicity requirements of metal-based catalytic antioxidants for high

dx.doi.org/10.1021/jm201233r | J. Med. Chem. 2011, 54, 8658−8669

activity in the carrageenan assay, we anticipated that bis-acetate **16a** would hydrolyze and clear more rapily than **16b** and **16c** (by producing the diol **15**, which could be easily metabolically conjugated or oxidized). From the data presented in Figure 6, bis-acetate **16a** produced a strong antihyperalgesic effect out to 2 h postcarrageenan, but the effect was lost at 3 h. Bis-propionate **16b** had a strong antihyperalgesic effect out to 3 h with a decline in this effect occurring in the 4−5 h time period. Finally, compound **16c**, the bis-isobutyrate, showed potent antihyperalgesic action out to the 5 h time point. If loss of activity in this assay can be explained by the clearance of these complexes from the sites of neuroinflammatory pain due to ester hydrolysis (affording increased sites of polarity/bioconjugation), then the results presented in Figure 6 are consistent with the anticipated rates of hydrolysis for this series of bis-ester complexes.

The real surprise came with compound **15**, the bis-*meso*-benzyl alcohol derivative (Figure 6). This compound performed the best in the series with excellent potency out to the 5 h time point. Thus, it is unlikely that the double hydrolyses of the bis-esters **16a−c** to the diol **15** are responsible for the observed clearance profile of these compounds. Partial hydrolysis of **16a−c** to afford the corresponding half alcohol-half ester derivative may be responsible for the observed clearance trend and would still depend upon the known hydrolysis rates for α-substituted esters. It is possible that the diol functionality increases the solubility of **15** enough to enhance oral absorption and bioaccumulation in the sites of inflammation, and this is responsible for the unexpected excellent in vivo performance of this molecule. Determination of the absolute bioavailability of selected members of this new family of Mn(III)-TCHP catalysts will be the subject of future studies.

Chronic Neuropathic Pain. To extend the therapeutic utility of novel and orally bioavailable "SO-sparing" Mn(III)-TCHPs in chronic pain states of different etiologies, we investigated the pharmacological effects of catalyst **7** in a well-characterized model of murine neuropathic pain caused by traumatic nerve injury, namely, chronic constriction injury (CCI) of the sciatic nerve.[76] The CCI model is a standard model used to screen novel non-narcotic agents in chronic neuropathic pain. As tested 7 days after surgery (time of maximal mechano-allodynia), constriction of the sciatic nerve in mice led to significant ($P < 0.05$) reduction in mechanical mean absolute paw-withdrawal thresholds (grams, g) at forces that failed to elicit withdrawal responses before constriction (baseline) in ipsilateral, but not contralateral, paws, indicative of the development of mechano-allodynia. Oral administration of **7** (10−100 mg/kg, $n = 4$; Figure 7) at the time of peak mechano-allodynia led to a rapid, dose-dependent, and near-to-maximal reversal of neuropathic pain within 1 h postdosing (Figure 7). Catalyst **7** had no effect on the withdrawal responses taken from contralateral paws. The ED_{50} of **7** as calculated at the time of peak reversal of mechano-allodynia was 28 mg/kg ($n = 4$, 95% CI = 15.64−51.67 mg/kg/day).

Conclusions. The traditional multifaceted drug regimens for controlling chronic pain are marginally effective and produce highly variable results depending upon the conditions of the contributing pathology.[77] Both chronic inflammatory and neuropathic pain states are therefore often difficult to treat in the clinic due to insufficient understanding of the nociceptive pathways involved.[77] While nonsteroidal anti-inflammatory drugs (NSAIDs) are a first-choice therapy for the management

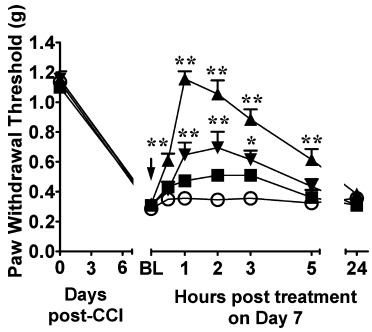

Figure 7. Mn(III)-TCHP **7** reverses neuropathic pain in a dose-dependent manner. When compared to vehicle (○; $n = 6$), oral Mn(III)-TCHP **7** (10, ■; 30, ▼; or 100 mg/kg, ▲; $n = 4$, arrow) reversed the tactile allodynia observed on D7 after CCI in a dose- and time-dependent manner. Mean ± SEM; n rats; ANOVA with Bonferroni corrections. $^*P < 0.01$, and $^{**}P < 0.001$ vs vehicle.

of arthritis pain, their well-known gastrointestinal side effects are of serious concern for chronic therapy. Despite the promise of COX-2 inhibitors as effective analgesics with reduced gastrointestinal side effects, the potential for severe cardiovascular side effects has prompted a critical review of these drugs.[78,79] These approaches suffer from being downstream from a key proinflammatory and neurotoxic biochemical pathway, which generates the hyperexcitatory conditions involved in transitioning acute to chronic pain and the maintenance of that inflammatory pain state. The linchpin molecule is peroxynitrite.[38−40] Peroxynitrite is a pro-inflammatory and pro-apoptotic species that also affects the nitration and modification of protein functions critical to neuronal homeostasis.[39,40] In that the overproduction of peroxynitrite and its subsequent destructive reactivity manifold lies at the heart of pain of various etiologies, molecules that can accomplish the direct scavenging or reduction of PN will provide a novel and analgesic and anti-inflammatory strategy.[38−40,74,80] Herein, we have shown that by employing a metal charge-shielding design concept, Mn(III)TCHP systems have been developed as orally active and selective PNR catalysts. These Mn(III)TCHP complexes have been shown to rapidly destroy peroxynitrite with minimal activity toward superoxide. The prototype compound **7** has been shown to be quite potent in models of inflammatory and neuropathic pain when dosed orally. Another promising aspect of this catalytic antioxidant strategy is that since the manganese atom is the center of activity in destroying peroxynitrite, the periphery of the porphyrin ligand system can be manipulated synthetically for optimization of in vivo performance. Thus, we have shown via a bis-*meso*-benzylalcohol/ester series (**15** and **16a−c**) that high in vivo activity can be maintained while tailoring clearance properties through functionalization of the ligand periphery.

■ EXPERIMENTAL SECTION

General Methods. Analytical thin-layer chromatography (TLC) was performed on Analtech 0.15 mm silica gel 60-GF254 plates. Visualization was accomplished with exposure to UV light or exposure to iodine. Solvents for extraction were HPLC or ACS grade. Chromatography was performed by the method of Still with Merck silica gel 60 (230−400 mesh) with the indicated solvent system. NMR spectra were collected on a JEOL ECS 400. ^{1}H NMR spectra were reported in ppm from tetramethylsilane on the δ scale. Data are reported as follows: chemical shift, multiplicity (s = singlet, d = doublet, t = triplet, q = quartet, m = multiplet, b = broadened, and

dx.doi.org/10.1021/jm201233r | J. Med. Chem. 2011, 54, 8658−8669

obs = obscured), coupling constants (Hz), and assignments or relative integration. ^{13}C NMR spectra were reported in ppm from the central deuterated solvent peak. Data are reported as follows: chemical shift, multiplicity, coupling information, and integration. Grouped shifts are provided where an ambiguity has not been resolved. LC-MS were run on a Waters Alliance−SQ 3100 system using Agilent Eclipse (XDB-C18, 4.6 mm × 150 mm, 5-Micron) column. All compounds tested in animals were deemed to be of >95% purity by LC-MS methods. UV−vis spectra were recorded using an Ocean Optics Red Tide UV−vis Spectrometer. The general procedures and apparatus for the electrochemistry experiments have been previously reported.[81]

Mn(III)-TCHP Chloride (7). A mixture of TCHP (100 mg, 0.19 mmol) in $CHCl_3$/MeOH (3:1, 60 mL) was treated with $MnCl_2$ (362 mg, 2.88 mmol) and 2,6-lutidine (1 mL). The mixture was stirred, open to the air, at room temperature for 1 h. The mixture was diluted with dichloromethane (150 mL), transferred to a separatory funnel, and washed with brine (150 mL). The layers were separated, and the organic solution was dried (Na_2SO_4), filtered, and concentrated. The residue was purified by alumina flash column chromatography, using dichloromethane as the eluent, and the desired complex **7** was collected as a brown solid (104 mg, 89% yield). LC-MS (85−95% acetonitrile in 0.05% TFA over 10 min) retention time = 3.23 min, $(M - Cl)^+$ = 579. HRMS (Q-TOF) m/z = 579.2314 (579.2315 calcd for $C_{36}H_{36}MnN_4$ $[M - Cl]^+$). UV/vis (1.0×10^{-5} M, CH_3OH) λ_{max} (log ε) 363 (4.95), 389 (sh), 457 (4.67), 543 (3.83), 574 (3.65).

Mn(III)-5,15-diphenyl-TCHP Chloride (10). Compound **10** was prepared from 5,15-bis-phenyl-TCHP (100 mg, 0.14 mmol) following the above method. Purification by flash chromatography [neutral alumina, CH_2Cl_2/MeOH (99:1)] afforded complex **10** as a brown solid (104 mg, 97% yield). LC-MS (85−95% acetonitrile in 0.05% TFA over 10 min) retention time = 5.73 min, $C_{48}H_{44}MnN_4$, $(M - Cl)^+$ = 731. HRMS (Q-TOF) m/z = 731.2934 (731.2941 calcd for $C_{48}H_{44}MnN_4$ $[M - Cl]^+$). UV/vis (1.0×10^{-5} M, CH_3OH) λ_{max} (log ε) 373 (4.85), 396 (sh), 465 (4.73), 554 (3.85), 586 (sh).

Mn(III)-5,10,15,25-tetrakis-phenyl-TCHP Chloride (12). Compound **12** was prepared from 5,10,15,25-tetrakis-phenyl-TCHP (100 mg, 0.12 mmol) following the above method. Purification by flash chromatography [neutral alumina, CH_2Cl_2/MeOH (98:2)] afforded complex **12** as a brown solid (96.0 mg, 87%). LC-MS (95−100% acetonitrile in 0.05% TFA over 10 min) retention time = 6.48 min, $C_{60}H_{52}MnN_4$, $(M - Cl)^+$ = 883. HRMS (Q-TOF) m/z = 883.3562 (883.3567 calcd for $C_{60}H_{52}MnN_4$ $[M - Cl]^+$). UV/vis (1.0×10^{-5} M, CH_3OH) λ_{max} (log ε) 386 (4.54), 408 (sh), 478 (4.72), 570 (3.69), 606 (sh).

5,15-Bis(4-hydroxymethyl)phenyl-TCHP (14). Into a dry 250 mL round-bottom flask fitted with a magnetic stirrer and an injection port with a rubber syringe cap under argon was added the diester porphyrin **13** (0.700 g, 0.880 mmol) and dry tetrahydrofuran (THF) (60 mL). To this stirred solution, maintained at 0 °C in an ice bath, was added $LiAlH_4$ (3.00 mL of a 1.0 M solution, 3.00 mmol). The mixture was allowed to warm to room temperature and then heated to 50 °C and stirred for 2 h. During this time, the progress of the reaction was followed by LC-MS. When the reaction was complete, the mixture was cooled and carefully quenched with water. After the mixture was partitioned with CH_2Cl_2 (200 mL) and water (200 mL), the desired purple product precipitated. The precipitate was collected by filtration and dried under vacuum to give compound **14** as a dark purple solid (0.59 g, 90% yield). ^1H NMR ($CDCl_3$): δ −2.39 (s, 4H), 1.68 (br m, 8H), 2.25 (br m, 8H), 2.45 (s, 4H), 2.64 (br m, 8H), 3.88 (s, 8H), 5.52 (br s, 2H), 7.90 (br m, 4H), 8.27 (br m, 4H), 10.56 (s, 2H). ^{13}C NMR ($CDCl_3$): δ 19.10, 22.29, 23.32, 23.75, 25.44, 56.56, 63.12, 67.50, 98.19, 119.08, 126.96, 135.51, 136.74, 137.57, 139.21, 140.79, 142.86, 145.43. LC-MS (50−95% acetonitrile in 0.05% TFA over 6 min) retention time = 4.03 min, $C_{50}H_{50}N_4O_2$, $(M + H)^+$ = 739.

Mn(III)-5,15-bis(4-hydroxymethyl)phenyl-TCHP (15). A solution of **14** (0.400 g, 0.541 mmol) in $CHCl_3$/MeOH (2:1, 45 mL) was treated with $MnCl_2$ (1.08 g, 8.66 mmol, 16 equiv) and 2,6-lutidine (1 mL). The mixture was stirred, open to the air, at 50 °C for 24 h. Removal of the solvent yielded a dark purple residue, which upon silica gel chromatography [eluent: $CHCl_3$/ MeOH (10:1)] afforded a dark purple solid complex **15** (0.33 g, 74% yield). LC-MS (50−95% acetonitrile in 0.05% TFA over 6 min) retention time = 6.55 min, $C_{50}H_{48}MnN_4O_2$, $(M - Cl)^+$ = 791. HRMS (Q-TOF) m/z = 791.3186 (791.3152 calcd for $C_{50}H_{48}MnN_4O_2$ $(M - Cl)^+$). UV/vis (1.0×10^{-5} M, CH_3OH) λ_{max} (log ε) 372 (4.52), 395 (sh), 464 (4.42), 551 (3.31), 582 (sh).

Mn(III)-5,15-bis(4-acetoxymethyl)phenyl-TCHP (16a). To a mixture of **6** (0.100 g, 0.121 mmol) and DMF (15 mL) was added acetic anhydride (3 mL, 31.7 mmol). The reaction was stirred at 60−70 °C for 3 h. The solvent was evaporated, and the residue was partitioned with CH_2Cl_2 (100 mL) and brine (50 mL). The layers were separated, and the CH_2Cl_2 solution was dried over Na_2SO_4, filtered, and concentrated to afford complex **16a** as a dark red solid (0.10 g, 91%). LC-MS (75−95% acetonitrile in 0.05% TFA over 6 min) retention time = 6.33 min, $C_{54}H_{52}MnN_4O_2$, $[M - Cl]^+$ = 875. HRMS (Q-TOF) m/z = 875.3397 (875.3364 calcd for $C_{54}H_{52}MnN_4O_2$, $[M - Cl]^+$). UV/vis (1.0×10^{-5} M, CH_3OH) λ_{max} (log ε) 372 (4.33), 394 (sh), 464 (4.25), 551 (3.30), 580 (sh).

Mn(III)-5,15-bis(4-propionyloxymethyl)phenyl-TCHP (16b). To a mixture of **6** (0.1 g, 0.120 mmol) and DMF (15 mL) was added propionic anhydride (3.00 mL, 23.4 mmol, 195 equiv). The reaction was stirred at 60−70 °C for 4 h. The solvent was evaporated, and the residue was partitioned with CH_2Cl_2 (100 mL) and brine (50 mL). The layers were separated, and the CH_2Cl_2 solution was dried over Na_2SO_4, filtered, and concentrated to afford complex **16b** as a dark red solid (95 mg, 84%). LC-MS (75−95% acetonitrile in 0.05% TFA over 6 min) retention time = 7.27 min, $C_{56}H_{56}MnN_4O_4$, $[M - Cl]^+$ = 903. HRMS (Q-TOF) m/z = 903.3705 (903.3676 calcd for $C_{56}H_{56}MnN_4O_4$, $[M - Cl]^+$). UV/vis (1.0×10^{-5} M, CH_3OH) λ_{max} (log ε) 373 (4.96), 394 (sh), 464 (4.86), 551 (3.96), 581 (sh).

Mn(III)-5,15-bis(4-isobutyryloxymethyl)phenyl-TCHP (16c). To a mixture of **6** (0.100 g, 0.120 mmol) and DMF (15 mL) were added isobutyric anhydride (3 mL, 18.0 mmol, 150 equiv) and DMAP (50 mg, 0.409 mmol). The reaction was stirred at 70 °C for 4 h. The solvent was evaporated, and the residue was partitioned with CH_2Cl_2 (100 mL) and brine (50 mL). The layers were separated, and the CH_2Cl_2 solution was dried over Na_2SO_4, filtered, and concentrated to afford complex **16c** as a dark red solid (0.10 g, 85%). LC-MS (50−95% acetonitrile in 0.05% TFA over 10 min) retention time = 8.47 min, $C_{58}H_{60}MnN_4O_4$, $[M - Cl]^+$ = 931. HRMS (Q-TOF) m/z = 931.4011 (931.3990 calcd for $C_{58}H_{60}MnN_4O_4$, $[M - Cl]^+$). UV/vis (1.0×10^{-5} M, CH_3OH) λ_{max} (log ε) 373 (4.76), 394 (sh), 464 (4.66), 551 (3.68), 581 (sh).

Inhibition of Aryl Boronate Oxidation Assay. Stock solutions of 4-acetylphenylboronic acid and the PNR catalyst were prepared in DMSO (in the 5−50 mM range). Peroxynitrite in 0.1 N NaOH solution was kept frozen at −80 °C until needed (see the Supporting Information). Small aliquots of the PN solution were thawed and kept on ice, and the concentration was measured by UV spectroscopy (λ_{max} = 302 nm; ε = 1670 M^{-1} cm^{-1}) just before measurements were made. Peroxynitrite concentrations ranged from 58 to 77 mM for these studies. In a typical procedure, 9.5×10^{-7} mol of 4-acetoxyphenylboronic acid (24.0 μL of stock) was dispensed into a small vial equipped with a magnetic stir bar. A 1.00 mL amount of 250 mM phosphate buffer (pH = 7.2), which contained 0.7% sodium dodecyl sulfate and 100 μM DTPA, was added followed by 9.5×10^{-7} mol of the PNR catalyst (aliquot from DMSO stock). To this rapidly stirred mixture was added 9.5×10^{-7} mol of peroxynitrite by rapid injection. The mixture was stirred for 1 min and analyzed by LC-MS [Waters Alliance-MS3100 system; 15% acetonitrile/H_2O to 95% acetonitrile (0.05% TFA) over 10 min; Agilent Eclipse XD8-C18 column, 5 μM, 4.6 mm × 150 mm, UV detection 280 nm for 4-hydroxyacetophenone oxidation product]. Reactions were run in triplicate and compared to controls (also run in triplicate), which contained everything except the PNR catalyst (amounts of DMSO that were equivalent to those from aliquoted PNR catalyst solutions were added to the controls to compensate for the very small effect of DMSO). The peak areas for the phenol oxidation product were compared for catalyst versus control runs to determine percent inhibition.

CCI Model of Neuropathic Pain (CCI). CCI to the sciatic nerve of the left hind leg in mice was performed under general anesthesia using the Bennett model.[76] Briefly, mice (weighing 25−30 g at the time of surgery) were anesthetized with 3% isoflurane/100% O_2 inhalation and maintained on 2% isoflurane/100% O_2 for the duration of surgery. The left thigh was shaved and scrubbed with chlorohexidine, and a small incision (1−1.5 cm in length) was made in the middle of the lateral aspect of the left thigh to expose the sciatic nerve. The nerve was loosely ligated at two distinct sites (spaced at a 2 mm interval) around the entire diameter of the nerve using silk sutures (6.0). The surgical site was closed with a single muscle suture and a skin clip. In this model, maximal tactile allodynia is established between day 5−7 and lasts for at least 1−2 months after surgery. On day 0 (baseline, BL), mechanical withdrawal thresholds were assessed by the von Frey test before surgery and subsequently on day 8 postsurgery. To examine changes in baseline nociceptive responses to tactile stimulation, animals were placed in elevated cages with a wire mesh floor and allowed to acclimate for 15 min. The plantar aspect of hindpaws was probed with calibrated von Frey filaments (0.07, 0.16, 0.40, 1.00, and 2.00 g) purchased from Stoelting (Wood Dale, IL) according to the up and down method.[82] The mechanical threshold was assessed three times at each time point to yield a mean value, which is reported as mean absolute threshold (grams, g). The development of mechano-allodynia is evidenced by a significant ($P < 0.05$) reduction in mechanical paw-withdrawal thresholds (grams, g) at forces that fail to elicit withdrawal responses before CCI baseline.

Carrageenan-Induced Thermal Hyperalgesia. Lightly anesthetized rats [CO_2 (80%)/O_2 (20%)] received a subplantar injection of carrageenan (50 μL of a 1% solution in saline) or its vehicle (50 μL saline) into the right hindpaw. Drugs or their vehicle were given by gavage or by intraperitoneal injection (0.2 mL) 30 min before carrageenan or its vehicle. Hyperalgesic responses to heat were determined by the Hargreaves' Method using a Basile Plantar Test (Ugo Basile; Comeria, Italy)[72] with a cutoff latency of 20 s employed to prevent tissue damage. Rats were individually confined to Plexiglas chambers. A mobile infrared generator was positioned to deliver a thermal stimulus directly to an individual hindpaw from beneath the chamber. The withdrawal latency period of injected paws was determined with an electronic clock circuit and thermocouple. Results are expressed as Paw-Withdrawal Latency Change (s). Experiments were conducted with the experimenters blinded to treatment conditions.

■ ASSOCIATED CONTENT

Supporting Information

Information for the synthesis and characterization of compounds **7**-ligand, **8**-, **9**-, and **10**-ligand, and **12**-ligand; procedure and analysis methods for the inhibition of aryl boronate oxidation assay; animal welfare protocol and thermal hyperalgesia assay methods. This material is available free of charge via the Internet at http://pubs.acs.org.

■ AUTHOR INFORMATION

Corresponding Author

*Tel: 618-650-5088. Fax: 618-650-5145. E-mail: wneuman@siue.edu.

■ ACKNOWLEDGMENTS

Support of this research by the NIH (NIAMS, RC1AR058231) and NSF (CHE-0911537) is gratefully acknowledged. We thank the Donald Danforth Plant Science Center Proteomics and Mass Spectrometry Group and the Washington University Resource for Biomedical and Biological Mass Spectrometry for HRMS analysis.

■ REFERENCES

(1) Batinic-Haberle, I.; Reboucas, J. S.; Spasojevic, I. Superoxide dismutase mimics: chemistry, pharmacology, and therapeutic potential. *Antioxid. Redox Signaling* **2011**, *13*, 877−918.
(2) Ferrer-Sueta, G.; Radi, R. Chemical biology of peroxynitrite: Kinetics, diffusion, and radicals. *ACS Chem. Biol.* **2009**, *4*, 161−177.
(3) Di Napoli, M.; Papa, F. M-40403 Metaphore Pharmaceuticals. *IDrugs* **2005**, *8*, 67−76.
(4) Riley, D. P.; Neumann, W. L.; Henke, S. L.; Lennon, P.; Aston, K.; Salvemini, D.; Sikorski, J. A.; Fobian, Y. M.; Grapperhaus, M. L.; Kusturin, C. L. Substituted pyridino pentaazamacrocycle complexes having superoxide dismutase activity as therapeutic agents. U.S. Patent 6214817, 2001.
(5) Salvemini, D.; Riley, D. P. Nonpeptidyl mimetics of superoxide dismutase in clinical therapies for diseases. *Cell. Mol. Life Sci.* **2000**, *57*, 1489−1492.
(6) Doctrow, S. R.; Baudry, M.; Huffman, K.; Malfroy, B.; Melov, S. Salen manganese complexes: Multifuncional catalytic antioxidants protective in models of neurodegenerative diseases of aging. *ACS Symp. Ser.* **2005**, *903*, 319−347.
(7) Salvemini, D.; Muscoli, C.; Riley, D. P.; Cuzzocrea, S. Superoxide dismutase mimetics. *Pulm. Pharmacol. Ther.* **2002**, *15*, 439−447.
(8) Salvemini, D.; Riley, D. P.; Cuzzocrea, S. SOD mimetics are coming of age. *Nature Rev.* **2002**, *1*, 367−374.
(9) Peng, J.; Stevenson, F. F.; Doctrow, S. R.; Andersen, J. K. Superoxide dismutase/catalase mimetics are neuroprotective against selective paraquat-mediated dopaminergic neuron death in the substantial nigra: Implications for Parkinson disease. *J. Biol. Chem.* **2005**, *280*, 29194−29198.
(10) Sharpe, M. A.; Ollosson, R.; Stewart, V. C.; Clark, J. B. Oxidation of nitric oxide by oxomanganese-salen complexes: a new mechanism for cellular protection by superoxide dismutase/catalase mimetics. *Biochem. J.* **2002**, *366*, 97−107.
(11) Lee, J. H.; Julianne, A.; Groves, J. T. Rapid decomposition of peroxynitrite by manganese porphyrin-antioxidant redox couples. *Bioorg. Med. Chem. Lett.* **1997**, *7*, 2913−2918.
(12) Lee, J. H.; Julianne, A.; Groves, J. T. Manganese Porphyrins as Redox-Coupled Peroxynitrite Reductases. *J. Am. Chem. Soc.* **1998**, *120*, 6053−6061.
(13) Shimanovich, R.; Groves, J. T. Mechanisms of peroxynitrite decomposition catalyzed by FeTMPS, a bioactive sulfonated iron porphyrin. *Arch. Biochem. Biophys.* **2001**, *387*, 307−317.
(14) Mahammed, A.; Gross, Z. Iron and manganese corroles are potent catalysts for the decomposition of peroxynitrite. *Angew. Chem., Int. Ed. Engl.* **2006**, *45*, 6544−6547.
(15) Okun, Z.; Kupershmidt, L.; Amit, T.; Mandel, S.; Bar-Am, O.; Youdim, M. B.; Gross, Z. Manganese corroles prevent intracellular nitration and subsequent death of insulin-producing cells. *ACS Chem. Biol.* **2009**, *4*, 910−914.
(16) Kanamori, A.; Catrinescu, M. M.; Mahammed, A.; Gross, Z.; Levin, L. A. Neuroprotection against superoxide anion radical by metallocorroles in cellular and murine models of optic neuropathy. *J. Neurochem.* **2011**, *114*, 488−498.
(17) Kupershmidt, L.; Okun, Z.; Amit, T.; Mandel, S.; Saltsman, I.; Mahammed, A.; Bar-Am, O.; Gross, Z.; Youdim, M. B. Metallocorroles as cytoprotective agents against oxidative and nitrative stress in cellular models of neurodegeneration. *J. Neurochem.* **2010**, *113*, 363−373.
(18) Haber, A.; Mahammed, A.; Fuhrman, B.; Volkova, N.; Coleman, R.; Hayek, T.; Aviram, M.; Gross, Z. Amphiphilic/Bipolar metallocorroles that catalyze the decomposition of reactive oxygen and nitrogen species, rescue lipoproteins from oxidative damage, and attenuate atherosclerosis in mice. *Angew. Chem., Int. Ed. Engl.* **2008**, *47*, 7896−7900.
(19) Eckshtain, M.; Zilbermann, I.; Mahammed, A.; Saltsman, I.; Okun, Z.; Maimon, E.; Cohen, H.; Meyerstein, D.; Gross, Z. Superoxide dismutase activity of corrole metal complexes. *Dalton Trans.* **2009**, 7879−7882.
(20) McCord, J. M.; Fridovich, I. The reduction of cytochrome c by milk xanthine oxidase. *J. Biol. Chem.* **1968**, *243*, 5753−5760.

(21) McCord, J. M.; Fridovich, I. Superoxide dismutase. An enzymic function for erythrocuprein (hemocuprein). *J. Biol. Chem.* **1969**, *244*, 6049−6055.
(22) McCord, J. M.; Fridovich, I. The utility of superoxide dismutase in studying free radical reactions. I. Radicals generated by the interaction of sulfite, dimethyl sulfoxide, and oxygen. *J. Biol. Chem.* **1969**, *244*, 6056−6063.
(23) Faulkner, K. M.; Liochev, S. I.; Fridovich, I. Stable Mn(III) porphyrins mimic superoxide dismutase in vitro and substitute for it in vivo. *J. Biol. Chem.* **1994**, *269*, 23471−23476.
(24) Batinic-Haberle, I.; Rajic, Z.; Tovmasyan, A.; Reboucas, J. S.; Ye, X.; Leong, K. W.; Dewhirst, M. W.; Vujaskovic, Z.; Benov, L.; Spasojevic, I. Diverse functions of cationic Mn(III) N-substituted pyridylporphyrins, recognized as SOD mimics. *Free Radical Biol. Med.* **2011**, *51*, 1035−1053.
(25) Reboucas, J. S.; DeFreitas-Silva, G.; Spasojevic, I.; Idemori, Y. M.; Benov, L.; Batinic-Haberle, I. Impact of electrostatics in redox modulation of oxidative stress by Mn porphyrins: protection of SOD-deficient *Escherichia coli* via alternative mechanism where Mn porphyrin acts as a Mn carrier. *Free Radical Biol. Med.* **2008**, *45*, 201−210.
(26) Batinic-Haberle, I.; Spasojevic, I.; Fridovich, I. Tetrahydrobiopterin rapidly reduces the SOD mimic Mn(III) ortho-tetrakis(N-ethylpyridinium-2-yl)porphyrin. *Free Radical Biol. Med.* **2004**, *37*, 367−374.
(27) Ferrer-Sueta, G.; Hannibal, L.; Batinic-Haberle, I.; Radi, R. Reduction of manganese porphyrins by flavoenzymes and submitochondrial particles: A catalytic cycle for the reduction of peroxynitrite. *Free Radical Biol. Med.* **2006**, *41*, 503−512.
(28) Stern, M.; Jensen, M.; Kramer, K. Peroxynitrite decomposition catalysts. *J. Am. Chem. Soc.* **1996**, *118*, 8735−8736.
(29) Batinic-Haberle, I.; Spasojevic, I.; Hambright, P.; Benov, L.; Crumbliss, A.; Fridovich, I. Relationship among redox potentials, proton dissociation constants of pyrrolic nitrogens and in vivo and in vitro superoxide dismutating activities of manganese(III) and Iron(III) water-soluble porphyrins. *Inorg. Chem.* **1999**, *38*, 4011−4022.
(30) Ferrer-Sueta, G.; Batinic-Haberle, I.; Spasojevic, I.; Fridovich, I.; Radi, R. Catalytic scavenging of peroxynitrite by isomeric Mn(III) N-methylpyridylporphyrins in the presence of reductants. *Chem. Res. Toxicol.* **1999**, *12*, 442−449.
(31) Batinic-Haberle, I.; Benov, L.; Spasojevic, I.; Fridovich, I. The ortho effect makes manganese(III) meso-tetrakis(N-methylpyridinium-2-yl)porphyrin a powerful and potentially useful superoxide dismutase mimic. *J. Biol. Chem.* **1998**, *273*, 24521−24528.
(32) Spasojevic, I.; Chen, Y.; Noel, T. J.; Yu, Y.; Cole, M. P.; Zhang, L.; Zhao, Y.; Clair, D. K. St; Batinic-Haberle, I. Mn porphyrin-based superoxide dismutase (SOD) mimic, MnIIITE-2-PyP5+, targets mouse heart mitochondria. *Free Radical Biol. Med.* **2007**, *42*, 1193−1200.
(33) Batinic-Haberle, I.; Ndengele, M. M.; Cuzzocrea, S.; Reboucas, J. S.; Spasojevic, I.; Salvemini, D. Lipophilicity is a critical parameter that dominates the efficacy of metalloporphyrins in blocking the development of morphine antinociceptive tolerance through peroxynitrite-mediated pathways. *Free Radical Biol. Med.* **2009**, *46*, 212−219.
(34) Kos, I.; Reboucas, J. S.; DeFreitas-Silva, G.; Salvemini, D.; Vujaskovic, Z.; Dewhirst, M. W.; Spasojevic, I.; Batinic-Haberle, I. Lipophilicity of potent porphyrin-based antioxidants: Comparison of ortho and meta isomers of Mn(III) N-alkylpyridylporphyrins. *Free Radical Biol. Med.* **2009**, *47*, 72−78.
(35) Spasojevic, I.; Chen, Y.; Noel, T. J.; Fan, P.; Zhang, L.; Reboucas, J. S.; St. Clair, D. K.; Batinic-Haberle, I. Pharmacokinetics of the potent redox-modulating manganese porphyrin, MnTE-2-PyP(5+), in plasma and major organs of B6C3F1 mice. *Free Radical Biol. Med.* **2008**, *45*, 943−949.
(36) Liang, L. P.; Huang, J.; Fulton, R.; Day, B. J.; Patel, M. An orally active catalytic metalloporphyrin protects against 1-methyl-4-phenyl-1,2,3,6-tetrahydropyridine neurotoxicity in vivo. *J. Neurosci.* **2007**, *27*, 4326−4333.
(37) Rosenthal, R. A.; Huffman, K. D.; Fisette, L. W.; Damphousse, C. A.; Callaway, W. B.; Malfroy, B.; Doctrow, S. R. Orally available Mn porphyrins with superoxide dismutase and catalase activities. *J. Biol. Inorg. Chem.* **2009**, *14*, 979−991.
(38) Salvemini, D.; Little, J. W.; Doyle, T.; Neumann, W. L. Roles of reactive oxygen and nitrogen species in pain. *Free Radical Biol. Med.* **2011**, *51*, 951−966.
(39) Salvemini, D.; Neumann, W. L. Peroxynitrite: A strategic linchpin of opioid analgesic tolerance. *Trends Pharmacol. Sci.* **2009**, *30*, 194−202.
(40) Salvemini, D.; Neumann, B. Targeting peroxynitrite driven nitroxidative stress with synzymes: A novel therapeutic approach in chronic pain management. *Life Sci.* **2010**, *86*, 604−614.
(41) Kamat, N. P.; Liao, Z.; Moses, L. E.; Rawson, J.; Therien, M. J.; Dmochowski, I. J.; Hammer, D. A. Sensing membrane stress with near IR-emissive porphyrins. *Proc. Natl. Acad. Sci. U.S.A.* **2011**, *108*, 13984−13989.
(42) Drain, C. M.; Varotto, A.; Radivojevic, I. Self-organized porphyrinic materials. *Chem. Rev.* **2009**, *109*, 1630−1658.
(43) Gotz, D. C.; Bruhn, T.; Senge, M. O.; Bringmann, G. Synthesis and stereochemistry of highly unsymmetric beta,meso-linked porphyrin arrays. *J. Org. Chem.* **2009**, *74*, 8005−8020.
(44) Senge, M. O.; Fazekas, M.; Notaras, E.; Blau, W.; Zawadzka, M.; Locos, O.; Mhuircheartaigh, E. Nonlinear Optical Properties of Porphyrins. *Adv. Mater.* **2007**, *19*, 2737−2774.
(45) Filatov, M. A.; Lebedev, A. Y.; Vinogradov, S. A.; Cheprakov, A. V. Synthesis of 5,15-diaryltetrabenzoporphyrins. *J. Org. Chem.* **2008**, *73*, 4175−4185.
(46) Kelkar, S. S.; Reineke, T. M. Theranostics: Combining Imaging and Therapy. *Bioconjugate Chem.* **2011**, *22*, 1879−1903.
(47) Manivannan, E. C. Y.; Joshi, P.; Pandey, R. The role of porphyrin chemistry in tumor imaging and photodynamic therapy. *Chem. Soc. Rev.* **2011**, *40*, 340−362.
(48) Lebedev, A. Y.; Troxler, T.; Vinogradov, S. A. Design of Metalloporphyrin-Based Dendritic Nanoprobes for Two-Photon Microscopy of Oxygen. *J. Porphyrins Phthalocyanines* **2008**, *12*, 1261−1269.
(49) Menard, F.; Sol, V.; Ringot, C.; Granet, R.; Alves, S.; Morvan, C. L.; Queneau, Y.; Ono, N.; Krausz, P. Synthesis of tetraglucosyl- and tetrapolyamine-tetrabenzoporphyrin conjugates for an application in PDT. *Bioorg. Med. Chem.* **2009**, *17*, 7647−7657.
(50) Oncel, N. B. S. Ni(II)- and Vanadyloctaethylporphyrin Self-Assembled Layers Formed on Bare and 5-(Octadecyloxy)isophthalic Acid Covered Graphite. *Langmuir* **2009**, *25*, 9290−9295.
(51) Fuhrhop, J.-H.; Hosseinpour, D. Hexahydro-29H,31H-tetrabenzo[b,g,l,q]porphin and -octayl octaacetate. *Liebigs Ann. Chem.* **1985**, 689−695.
(52) May, D. Jr.; Lash, T. D. Porphyrins with exocyclic rings. 2. Synthesis of Geochemically Significant Tetrahydrobenzoporphyrins from 4,5,6,7-Tetrahydro-2H-Isoindoles. *J. Org. Chem.* **1992**, *57*, 4820−4828.
(53) Riley, D. P.; Neumann, W. L.; Henke, S. L.; Lennon, P. J.; Weiss, R. H. Synthesis, Characterization, and Stability of Manganese (II) C-Substituted 1,4,7,10,13 Pentaazacyclopentadecane Complexes Exhibiting Superoxide Dismutase Activity. *Inorg. Chem.* **1996**, *35*, 5213−5231.
(54) Riley, D. P.; Neumann, W. L.; Lennon, P. J.; Weiss, R. H. Toward the Rational Design of Superoxide Dismutase Mimics: Mechanistic Studies for the Elucidation of Substituent Effects on the Catalytic Activity of Macrocyclic Manganse(II) Complexes. *J. Am. Chem. Soc.* **1997**, *119*, 6522−6528.
(55) Ohnishi, M.; Urry, D. W. Solution conformation of valinomycin-potassium ion complex. *Science* **1970**, *168*, 1091−1092.
(56) Veber, D. F.; Johnson, S. R.; Cheng, H. Y.; Smith, B. R.; Ward, K. W.; Kopple, K. D. Molecular properties that influence the oral bioavailability of drug candidates. *J. Med. Chem.* **2002**, *45*, 2615−2623.
(57) Ono, N.; Hisayuki, K.; Bougauchi, M.; Maruyama, K. Porphyrin synthesis from nitro compounds. *Tetrahedron* **1990**, *46*, 7483−7496.

(58) Ono, N. Barton-Zard Pyrrole Synthesis and its Application to Synthesis of Porphyrins, Polypyrroles, and Dipyrromethene Dyes. *Heterocycles* **2008**, *75*, 243−284.
(59) Finikova, O. S.; Cheprakov, A. V.; Beletskaya, I. P.; Carroll, P. J.; Vinogradov, S. A. Novel versatile synthesis of substituted tetrabenzoporphyrins. *J. Org. Chem.* **2004**, *69*, 522−535.
(60) Lodge, K. Octanol-water partition coefficients of cyclic C-7 hydrocarbons and selected derivatives. *J. Chem. Eng. Data* **1999**, *44*, 1321−1324.
(61) Gentemann, S.; Medforth, C.; Forsyth, T. P.; Nurco, D. J.; Smith, K. M.; Fajer, J.; Holten, D. Photophysical properties of conformationally distorted metal-free porphyrins. Investigation into the deactivation mechanisms of the lowest excited singlet state. *J. Am. Chem. Soc.* **1994**, *116*, 7363−7368.
(62) Valko, K. Application of high-performance liquid chromatography based measurements of lipophilicity to model biological distribution. *J. Chromatogr., A* **2004**, *1037*, 299−310.
(63) Sikora, A.; Zielonka, J.; Lopez, M.; Joseph, J.; Kalyanaraman, B. Direct oxidation of boronates by peroxynitrite: mechanism and implications in fluorescence imaging of peroxynitrite. *Free Radical Biol. Med.* **2009**, *47*, 1401−1407.
(64) Trujillo, M.; Ferrer-Sueta, G.; Radi, R. Peroxynitrite detoxification and its biologic implications. *Antioxid. Redox Signaling* **2008**, *10*, 1607−1620.
(65) Szabo, C.; Ischiropoulos, H.; Radi, R. Peroxynitrite: Biochemistry, pathophysiology and development of therapeutics. *Nature Rev.* **2007**, *6*, 662−680.
(66) Hunt, J. A.; Lee, J.; Groves, J. T. Amphiphilic peroxynitrite decomposition catalysts in liposomal assemblies. *Chem. Biol.* **1997**, *4*, 845−858.
(67) Geiger, W. E. Organometallic Electrochemistry: Origins, Development, and Future. *Organometallics* **2007**, *26*, 5738−5765.
(68) Schultz, F. A.; Duncan, C. T.; Risgby, M. A. Electrochemistry of the group 7 elements: Manganese, technetium, and rhenium. In *The Encyclopedia of Electrochemistry: Inorganic Electrochemistry*; Bard, A. J., Stratman, M., Scholz, F., Pickett, C. J., Eds.; Wiley-VCH: Weinheim, 2006; Vol. *7b*, p 412.
(69) Radi, R. A.; Rubbo, H.; Prodanov, E. Comparison of the effects of superoxide dismutase and cytochrome c on luminol chemiluminescence produced by xanthine oxidase-catalyzed reactions. *Biochim. Biophys. Acta* **1989**, *994*, 89−93.
(70) Koppenol, W. H.; Moreno, J. J.; Pryor, W. A.; Ischiropoulos, H.; Beckman, J. S. Peroxynitrite, a cloaked oxidant formed by nitric oxide and superoxide. *Chem. Res. Toxicol.* **1992**, *5*, 834−842.
(71) Massaad, C. A.; Klann, E. Reactive Oxygen Species in the Regulation of Synaptic Plasticity and Memory. *Antioxid. Redox Signaling* **2011**, *14*, 2013−2054.
(72) Hargreaves, K.; Dubner, R.; Brown, F.; Flores, C.; Joris, J. A new and sensitive method for measuring thermal nociception in cutaneous hyperalgesia. *Pain* **1988**, *32*, 77−88.
(73) Salvemini, D.; Wang, Z. Q.; Bourdon, D. M.; Stern, M. K.; Currie, M. G.; Manning, P. T. Evidence of peroxynitrite involvement in the carrageenan-induced rat paw edema. *Eur. J. Pharmacol.* **1996**, *303*, 217−220.
(74) Salvemini, D. Peroxynitrite and opiate antinociceptive tolerance: a painful reality. *Arch. Biochem. Biophys.* **2009**, *484*, 238−244.
(75) Takahashi, H.; Tamagawa, S.; Sakano, H.; Katagi, T.; Mizuno, N. Effects of the ester moiety on stereoselective hydrolysis of several propranolol prodrugs in rat tissues. *Biol. Pharm. Bull.* **1995**, *18*, 1401−1404.
(76) Bennett, G. J.; Xie, Y. K. A peripheral mononeuropathy in rat that produces disorders of pain sensation like those seen in man. *Pain* **1988**, *33*, 87−107.
(77) Renfrey, S.; Downton, C.; Featherstone, J. The painful reality. *Nature Rev.* **2003**, *2*, 175−176.
(78) Grosser, T. The pharmacology of selective inhibition of COX-2. *Thromb. Haemostasis* **2006**, *96*, 393−400.
(79) Grosser, T.; Fries, S.; FitzGerald, G. A. Biological basis for the cardiovascular consequences of COX-2 inhibition: Therapeutic challenges and opportunities. *J. Clin. Invest.* **2006**, *116*, 4−15.
(80) Salvemini, D.; Batinic-Haberle, I.; Cuzzocrea, S.; Reboucas, J.; Masini, E.; Matuschak, G.; Spasojevic, I. Peroxynitrite decomposition catalysts as adjuncts to morphine for the management of chronic pain states. *FASEB J.* **2008**, *93*, 1126−1134.
(81) Shaw, M. J.; Afridi, S. J.; Light, S. L.; Mertz, J. N.; Ripperda, S. E. Synthesis and Electrochemistry of Iron-Pyrylium Complexes. *Organometallics* **2004**, *23*, 2778−2783.
(82) Dixon, W. J. Efficient analysis of experimental observations. *Annu. Rev. Pharmacol. Toxicol.* **1980**, *20*, 441−462.